

Energy transfer, pressure tensor and heating of kinetic plasma

Yan Yang,^{1,2} William H. Matthaeus,² Tulasi N. Parashar,² Colby C. Haggerty,² Vadim Roytershteyn,³ William Daughton,⁴ Minping Wan,⁵ Yipeng Shi,¹ and Shiyi Chen^{5,1}

¹*State Key Laboratory for Turbulence and Complex Systems,
Center for Applied Physics and Technology, College of Engineering,
Peking University, Beijing 100871, P. R. China*

²*Department of Physics and Astronomy,
University of Delaware, Newark, DE 19716*

³*Space Science Institute, Boulder CO, 80301*

⁴*Los Alamos National Laboratory, Los Alamos, NM 87545*

⁵*Department of Mechanics and Aerospace Engineering,
South University of Science and Technology of China,
Shenzhen, Guangdong 518055, China*

(Dated: March 12, 2018)

Abstract

Kinetic plasma turbulence cascade spans multiple scales ranging from macroscopic fluid flow to sub-electron scales. Mechanisms that dissipate large scale energy, terminate the inertial range cascade and convert kinetic energy into heat are hotly debated. Here we revisit these puzzles using fully kinetic simulation. By performing scale-dependent spatial filtering on the Vlasov equation, we extract information at prescribed scales and introduce several energy transfer functions. This approach allows highly inhomogeneous energy cascade to be quantified as it proceeds down to kinetic scales. The pressure work, $-(\mathbf{P} \cdot \nabla) \cdot \mathbf{u}$, can trigger a channel of the energy conversion between fluid flow and random motions, which is a collision-free generalization of the viscous dissipation in collisional fluid. Both the energy transfer and the pressure work are strongly correlated with velocity gradients.

I. INTRODUCTION

The classical energy cascade scenario is of great importance in explaining the heating of corona and solar wind [1–5]: In these applications, one envisions that significant amounts of energy reside in large-scale fluctuations. Nonlinear interactions cause a cascade that transports energy to smaller scales where dissipation occurs. At dissipation scales kinetic processes that absorb these energy fluxes, produce temperature enhancements. Inhomogeneities generated in this process may in turn be responsible for large scale flows, while also producing populations of energetic particles. Many systems, including low-collisionality astrophysical plasmas, may be well described by fluid theory at large scales. For plasmas, including electromagnetic fields, this large scale description would usually be taken to be some form of magnetohydrodynamics (MHD). The present paper is devoted to extending ideas about turbulence cascade into the deep kinetic range, so that we may develop a better understanding of turbulence cascade in low collisionality or even collisionless plasma.

It is reasonable to assume that MHD remains a credible approximation for a kinetic plasma at scales large enough to be well separated from kinetic effects. For that range, scale filtered analysis [6] shows how the fluid flow energy cascades almost conservatively from large to small scales, despite not being strictly an invariant of the MHD system. Then an important subsequent question asks how energy transfer proceeds down to kinetic scales as various kinetic processes come to the fore. The present paper addresses statistical properties of energy transfer across scales, recognizing the possible significance of energy cascade in explaining the heating and acceleration of the wind, and many other properties.

In this work we will avoid adopting familiar approaches that rely heavily on linear theory of waves, instabilities and damping rates [7–9], or on weak turbulence approaches that require a leading order description in terms of linear modes. Instead we consider the full Vlasov-Maxwell system, and employ a filtering approach that is familiar in hydrodynamics [10] and large-eddy simulation [11–15] communities but less used in kinetic plasma. Examining filtered equations for energy transfer, we can assess the relative importance of different transfer terms at all scales ranging from MHD to electron scales.

The present approach provides extensions of what fluid models tell us about the plasma cascade. In the context of plasma applications, MHD simulations adopt an *ad hoc* model of dissipation (e.g., viscous and resistive dissipation), rather than engaging the details of

the small dynamics that make up the plasma dissipation range. The turbulence in most astrophysical contexts, on the other hand, is typically of weak collisionality, and frequently modeled as collisionless, and thus collisional (viscous and resistive) dissipation at small scales cannot emerge immediately. While various specific processes may contribute to conversion of energy from fields into random degrees of freedom, for example, wave-particle interactions (WPI) [16–20] and processes associated with coherent structures (CS) [21–26], are likely ingredients, but nevertheless an explicit dissipation function cannot at this moment be defined clearly for a collisionless system.

Lacking such an explicit form for dissipation, Wan et al. [27] considered a surrogate dissipation measure related to the work done by the electromagnetic field on the plasma particles. Recent studies in compressible MHD turbulence [6, 28] demonstrated that, apart from collisional dissipation, the pressure dilatation, $-p\nabla \cdot \mathbf{u}$, can trigger an alternative channel of the conversion between kinetic and internal energy. Accordingly, one could expect that there might be an analogous role of the pressure tensor in collisionless plasma. In fact one expects pressure to be influential in at least several ways. On the one hand, the pressure term in anisotropic compressible turbulence moderates the competition and balance between two energy redistributive processes, i.e., return-to-isotropy [29, 30] and kinetic-potential (internal) energy equipartition [31–34]. On the other hand, the pressure tensor in kinetic plasmas plays a very important role in the force balance equations as well as in the generalized Ohm’s law near neutral lines [35, 36]. Here we show that the global energy exchange between fluid flow and particles (i.e., kinetic and thermal energies), derived from the Vlasov equation, is bridged immediately by the collaboration of pressure tensor and strain stress (i.e., velocity gradient). This possibly provides a new perspective on the collisionless dissipation mechanism and on the collisionless plasma cascade in general. The possible importance of pressure work in generating internal energy has been brought up in Ref. [37] (hereafter, Paper I). Here we extend that study and explore this novelty in a more comprehensive and detailed way.

II. GLOBAL ENERGY CONVERSION

Standard manipulation of the Vlasov equation yields macroscopic equations for plasma particles of type α in a collisionless plasma:

$$\partial_t \rho_\alpha + \nabla \cdot (\rho_\alpha \mathbf{u}_\alpha) = 0, \quad (1)$$

$$\partial_t (\rho_\alpha \mathbf{u}_\alpha) + \nabla \cdot (\rho_\alpha \mathbf{u}_\alpha \mathbf{u}_\alpha) = -\nabla \cdot \mathbf{P}_\alpha + n_\alpha q_\alpha (\mathbf{E} + \mathbf{u}_\alpha / c \times \mathbf{B}), \quad (2)$$

$$\partial_t \mathcal{E}_\alpha + \nabla \cdot (\mathcal{E}_\alpha \mathbf{u}_\alpha) = -\nabla \cdot (\mathbf{P}_\alpha \cdot \mathbf{u}_\alpha) - \nabla \cdot \mathbf{q}_\alpha + n_\alpha q_\alpha \mathbf{E} \cdot \mathbf{u}_\alpha. \quad (3)$$

Here $\rho_\alpha = m_\alpha n_\alpha$ represents the mass density; m_α is the mass of particles of species α ; n_α is the number density; \mathbf{u}_α gives the fluid flow (bulk) velocity; $n_\alpha q_\alpha$ represents the charge density; $\mathbf{P}_\alpha = m_\alpha \int (\mathbf{v} - \mathbf{u}_\alpha) (\mathbf{v} - \mathbf{u}_\alpha) f_\alpha(\mathbf{x}, \mathbf{v}, t) d\mathbf{v}$ is the pressure tensor; $\mathcal{E}_\alpha = \int \frac{1}{2} m_\alpha \mathbf{v}^2 f_\alpha(\mathbf{x}, \mathbf{v}, t) d\mathbf{v}$ is the total (average and random) kinetic energy; $\mathbf{q}_\alpha = \frac{1}{2} m_\alpha \int (\mathbf{v} - \mathbf{u}_\alpha)^2 (\mathbf{v} - \mathbf{u}_\alpha) f_\alpha(\mathbf{x}, \mathbf{v}, t) d\mathbf{v}$ is the heat flux vector.

Decomposing the total energy \mathcal{E}_α into average and random parts facilitates the understanding of energy converting processes. On defining the species fluid flow energy as $E_\alpha^f = \frac{1}{2} \rho_\alpha \mathbf{u}_\alpha^2$ and the thermal (random) energy as $E_\alpha^{th} = \frac{1}{2} m_\alpha \int (\mathbf{v} - \mathbf{u}_\alpha)^2 f_\alpha(\mathbf{x}, \mathbf{v}, t) d\mathbf{v}$, it is obvious that $\mathcal{E}_\alpha = E_\alpha^f + E_\alpha^{th}$. Computing the inner product of Eq. 2 with \mathbf{u}_α results in the fluid flow energy equation:

$$\partial_t E_\alpha^f + \nabla \cdot (E_\alpha^f \mathbf{u}_\alpha) = -\nabla \cdot (\mathbf{P}_\alpha \cdot \mathbf{u}_\alpha) + (\mathbf{P}_\alpha \cdot \nabla) \cdot \mathbf{u}_\alpha + n_\alpha q_\alpha \mathbf{E} \cdot \mathbf{u}_\alpha. \quad (4)$$

Subtracting Eq. 4 from Eq. 3 we obtain a time evolution equation for the random kinetic energy,

$$\partial_t E_\alpha^{th} + \nabla \cdot (E_\alpha^{th} \mathbf{u}_\alpha) = -(\mathbf{P}_\alpha \cdot \nabla) \cdot \mathbf{u}_\alpha - \nabla \cdot \mathbf{q}_\alpha. \quad (5)$$

Using the Maxwell curl equations, the equation governing electromagnetic energy, $E^m = \frac{1}{8\pi} (\mathbf{B}^2 + \mathbf{E}^2)$, can be written as:

$$\partial_t E^m + \frac{c}{4\pi} \nabla \cdot (\mathbf{E} \times \mathbf{B}) = -\mathbf{E} \cdot \mathbf{j} \quad (6)$$

where $\mathbf{j} = \sum_\alpha \mathbf{j}_\alpha$ is the total electric current density, and $\mathbf{j}_\alpha = n_\alpha q_\alpha \mathbf{u}_\alpha$ is the electric current density of species α . Under certain boundary conditions, e.g., periodic, integrating Eqs. 4, 5, and 6 over the whole volume, we can have

$$\partial_t \langle E_\alpha^f \rangle = \langle (\mathbf{P}_\alpha \cdot \nabla) \cdot \mathbf{u}_\alpha \rangle + \langle n_\alpha q_\alpha \mathbf{E} \cdot \mathbf{u}_\alpha \rangle, \quad (7)$$

$$\partial_t \langle E_\alpha^{th} \rangle = -\langle (\mathbf{P}_\alpha \cdot \nabla) \cdot \mathbf{u}_\alpha \rangle, \quad (8)$$

$$\partial_t \langle E^m \rangle = -\langle \mathbf{E} \cdot \mathbf{j} \rangle. \quad (9)$$

where $\langle \dots \rangle$ denotes a space average over the entire volume.

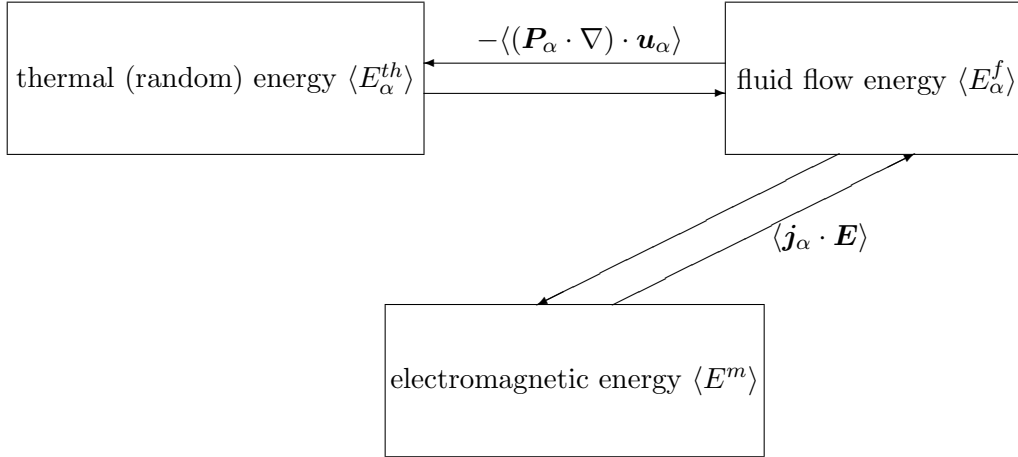


FIG. 1: Illustration of the available routes for global energy conversion. The point-wise values of $-(\mathbf{P}_\alpha \cdot \nabla) \cdot \mathbf{u}_\alpha$ and $\mathbf{j}_\alpha \cdot \mathbf{E}$ are not sign-definite. Therefore, there are two possible directions of energy conversion. $\langle \dots \rangle$ denotes the space average over the entire volume.

Fig. 1 illustrates the energy conversions as suggested by Eqs. 7, 8 and 9. One can see that for the collisionless case derived from the Vlasov equation, the pressure work, $-\langle (\mathbf{P}_\alpha \cdot \nabla) \cdot \mathbf{u}_\alpha \rangle$, is the only term converting fluid flow energy into thermal (random) energy, while the term, $\langle \mathbf{j}_\alpha \cdot \mathbf{E} \rangle$, represents the conversion between fluid flow and electromagnetic energies. The pressure work seems to be a more straightforward measure of heating rate when compared with electromagnetic work [27, 38]. At present, we cannot rule out the possibly strong correlation between the work done by pressure and work done by the electric field. For example, for a generalized Ohm's law, or the electron momentum equation, in the limit of massless electrons in collisionless plasma, we find that $\langle \mathbf{j}_e \cdot \mathbf{E} \rangle = -\langle (\mathbf{P}_e \cdot \nabla) \cdot \mathbf{u}_e \rangle$.

Notwithstanding that the pressure work is a general property in various fluid systems, seldom have studies investigated the role of pressure in modifying the thermal (random) energy in a turbulent kinetic plasma (however, see, e.g., Birn and Hesse [39], Birn *et al.* [40], Birn and Hesse [41]). In the realm of observations this is more or less due to the intractability of calculating velocity gradient from single spacecraft datasets and until recently, a lack of high cadence determination of the pressure tensor. These complication have led most observational studies of solar wind turbulence to rely on high cadence magnetic field data,

which is generally much more accessible. Even in simulation studies, accurate determination of the pressure tensor is challenging, requiring either large numbers of particles in PIC codes, or the use of computationally demanding Eulerian Vlasov simulations. Here we will use numerical simulations to explore the role of pressure tensor in heating of kinetic plasma in detail.

III. SIMULATION DETAILS

The fully kinetic particle-in-cell (PIC) simulation employed here spans from macroscopic fluid scales to kinetic scales. It is expedient for studies of energy transfer and dissipation. The simulation was performed using P3D code [42] in 2.5D geometry (three components of dependent field vectors and a two-dimensional spatial grid). Number density is normalized to the reference number density n_r (=1 in this simulation), mass to proton mass m_i (=1 in this simulation), and magnetic field to B_r (=1 in this run). Length is normalized to the ion inertial length d_i , time to the ion cyclotron time Ω_i^{-1} , and velocity to the reference Alfvén speed $v_{Ar} = B_r / (4\pi m_i n_r)^{1/2}$. Parameters of the PIC simulation are listed in Table I. It is conducted in periodic boundary conditions in both directions. The initial density, temperature and out-of-plane magnetic field B_0 are uniform. The initial v and b fluctuations are transverse to B_0 (“Alfvén mode”) and excited for prescribed wavenumbers with specified spectra and cross helicity. More details about the simulation can be found in Ref. Wu *et al.* [43].

TABLE I: Simulation parameters: box size L , grid points N^2 , mass ratio m_i/m_e , proton beta β_i , electron beta β_e , out of plane uniform magnetic field B_0 , the number of particles of each species per grid ppg and correlation scale λ_c .

Code	L	N^2	m_i/m_e	β_i	β_e	B_0	ppg	λ_c
P3D[42]	$102.4d_i$	8192^2	25	0.1	0.1	5.0	300	$16.8d_i$

We analyze statistics near the time of maximum root mean square(r.m.s.) electric current density (i.e., $t\Omega_i = 206.25$), shown by the dashed lines in Fig. 2(a). By this time the turbulence has fully developed and it has generated a complex pattern, characterized by sheet-like current structures spanning a range of scales as seen in Fig. 2(b). In order to

remove particle noise at grid scales, we apply a low-pass Fourier filter to the field data for $k\lambda_d > 1$ (Debye length λ_d) prior to statistical analyses. Demonstration of the efficacy of this filtering technique will be documented elsewhere [44].

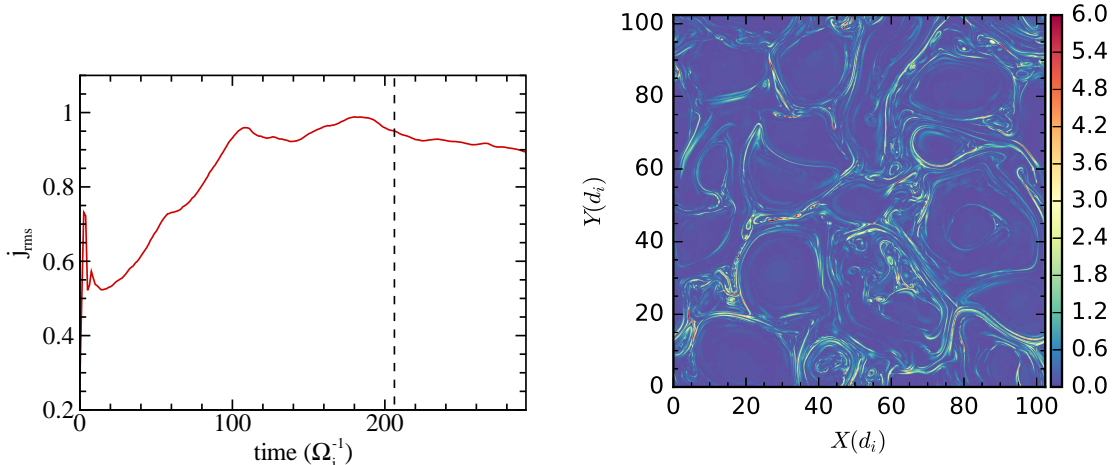


FIG. 2: (a) Time history of root mean square(r.m.s.) electric current density j_{rms} . The time snapshot ($t\Omega_i = 206.25$) near the maximum r.m.s. total electric current density, which is indicated by the dashed line, is analyzed. (b) Contour of the normalized second “invariant” of current density $Q_j = \frac{1}{4}\mathbf{j}^2/\langle\mathbf{j}^2\rangle$.

IV. ROLE OF PRESSURE TENSOR

A somewhat surprising result [37] further documented here is the correlation of pressure effects and dynamically appearing coherent structures associated with intermittency. In order to clarify the correlation between pressure tensor and intermittent structures, we split the pressure work, $-(\mathbf{P} \cdot \nabla) \cdot \mathbf{u}$, into two parts as follows. We suppress the subscript α for simplicity.

Decomposing the pressure tensor, $\mathbf{P} = (P_{ij})$, gives

$$P_{ij} = p\delta_{ij} + \Pi_{ij}, \quad (10)$$

where $p = \frac{1}{3}P_{ii}$ is the scalar pressure; a sum on repeated indexes is implied; δ_{ij} is the Kronecker delta; Π_{ij} is the remaining part with the scalar pressure subtracted from the pressure tensor, that is, the deviatoric pressure tensor.

The intrinsic decomposition of $\nabla\mathbf{u}$ into symmetric and anti-symmetric parts gives

$$\begin{aligned}\partial_i u_j &= S_{ij} + \Omega_{ij}, \\ &= \frac{1}{3}\theta\delta_{ij} + D_{ij} + \Omega_{ij},\end{aligned}\tag{11}$$

where $S_{ij} = \frac{1}{2}(\partial_i u_j + \partial_j u_i)$ and $\Omega_{ij} = \frac{1}{2}(\partial_i u_j - \partial_j u_i)$, with $\epsilon_{ijk}\Omega_{jk} = \omega_i$, are the strain-rate and rotation-rate tensors, respectively; ω_i is the vorticity; $\theta = S_{ii}$ is the dilatation; $D_{ij} = S_{ij} - \frac{1}{3}\theta\delta_{ij}$ is the traceless strain-rate tensor.

Using Eqs. 10 and 11, we can obtain

$$-(\mathbf{P} \cdot \nabla) \cdot \mathbf{u} = -p\theta - \Pi_{ij}D_{ij}.\tag{12}$$

One can see that $-p\theta$, accounting for compressive effects, is of the same form as the pressure dilatation in compressible MHD turbulence. The new term in kinetic plasma in comparison with MHD is $-\Pi_{ij}D_{ij}$, the double contraction of deviatoric pressure tensor and traceless strain-rate tensor. This term which will be called “*Pi-D*” hereafter is a salient feature of the present paper.

At this point we may recall that in the continuum formulation leading to the Navier-Stokes equations, with strong collisions, $-\Pi_{ij}$ actually is present, but rarely written in this way. Instead, in a Chapman-Enskog development, this term is equated with a viscous stress, which can then be expressed in terms of velocity gradient [45, 46]. In Sec. IV A, we will check whether the “*Pi-D*” term shares some properties with viscous dissipation.

Table II contains analysis based on the numerical simulation that compares $\langle -p\theta \rangle$ and $\langle -\Pi_{ij}D_{ij} \rangle$ and the electromagnetic work. One can see that the pressure dilatation is smaller as expected based on the weak compressibility in the run, where $\delta\rho'_\alpha/\langle\rho_\alpha\rangle = \sqrt{\langle(\rho_\alpha - \langle\rho_\alpha\rangle)^2\rangle}/\langle\rho_\alpha\rangle \simeq 0.12$. The $\langle -\Pi_{ij}D_{ij} \rangle$ terms are comparable to $\langle \mathbf{E} \cdot \mathbf{j}_\alpha \rangle$. Time average over about an electron gyroperiod is used in computing $\langle \mathbf{E} \cdot \mathbf{j}_\alpha \rangle$ to eliminate very high frequency oscillations.

To clarify the effect of the pressure tensor, we plot in Fig. 3(a) the contours of “*Pi-D*” for both electrons and ions. The “*Pi-D*” term contributes substantially to the energy exchange between the fluid flow and the random kinetic energy. These contributions are concentrated locally in space. The intensity and signs of “*Pi-D*” vary, so also do the amount and direction of the energy conversion. It is intermittent, while its net effect over the whole domain, i.e., its global average, is relatively small, which is also verified through the PDF plot in Fig.

TABLE II: Strength of global conversion of the fluid flow, thermal (random) and electromagnetic energies. All quantities are listed in the unit $v_{Ar}^3 d_i^{-1}$.

Species	$\langle -p\theta \rangle$	$\langle -\Pi_{ij} D_{ij} \rangle$	$\langle \mathbf{E} \cdot \mathbf{j}_\alpha \rangle$
Electron	0.0018	0.0045	0.0052
Ion	0.00075	0.0016	0.0016

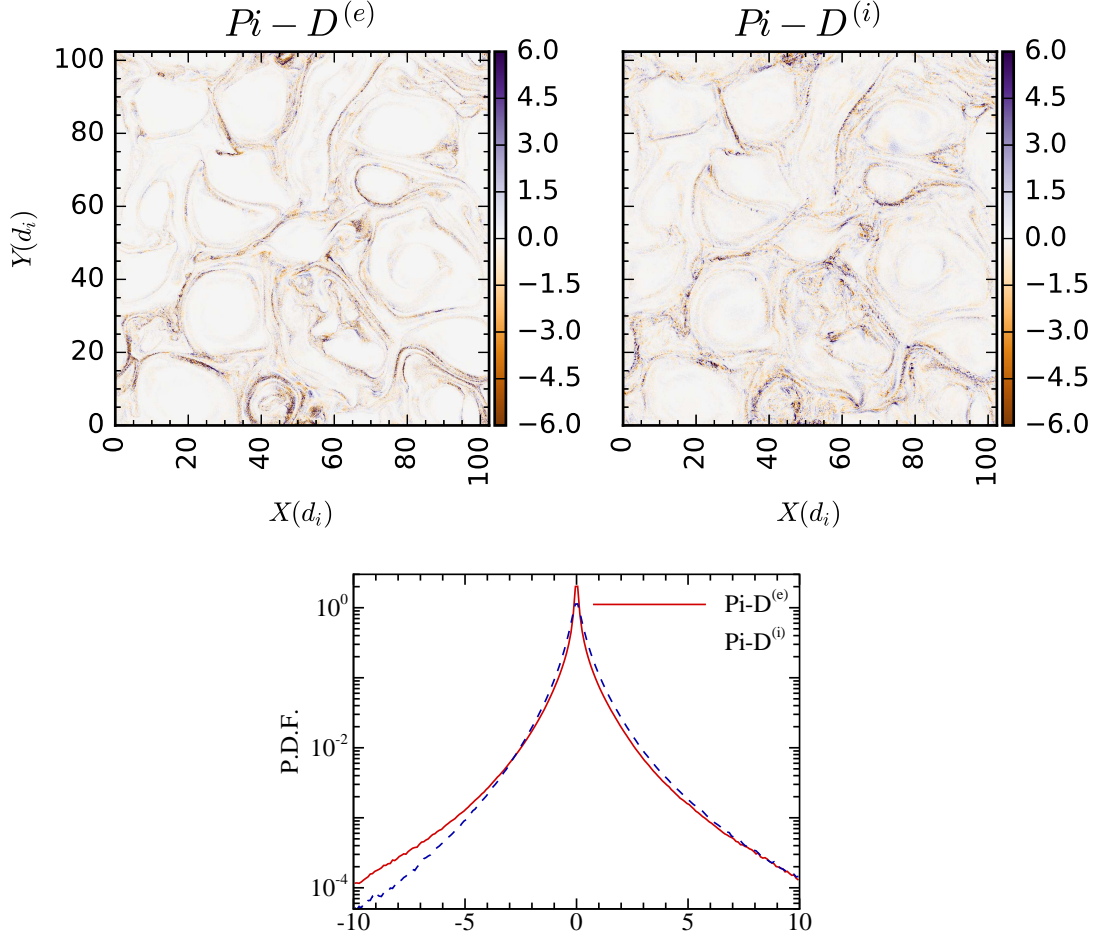


FIG. 3: (a) Contours of $-\Pi_{ij} D_{ij}$ for electrons (left) and ions (right) (reproduced from Paper I for completeness). Both quantities are normalized to their respective root mean square values. Both are organized into sheet-like structures. They are not sign-definite, thus the directions of energy conversion vary. (b) PDFs of normalized $-\Pi_{ij} D_{ij}$ of both electrons (red solid) and ions (blue dashed). They slightly tilt towards positive values, indicating that the fluid flow energy is converted into thermal (random) energy globally.

3(b). The long-tailed curves there slightly tilt towards positive values, i.e., the fluid flow energy is converted into thermal (random) energy globally.

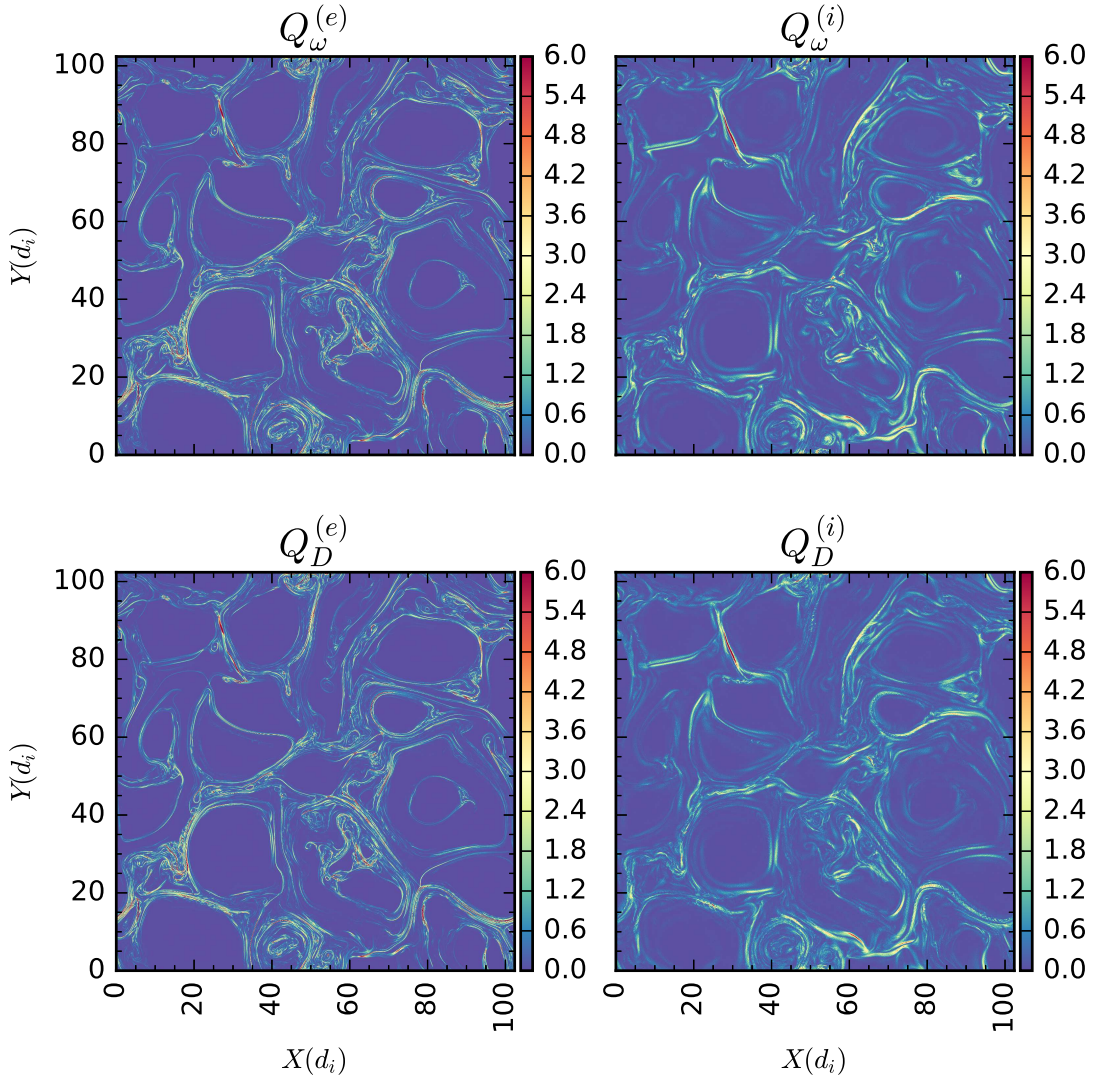


FIG. 4: Contours of the normalized second invariant of the rotation-rate tensor, (top row), $Q_\omega = \frac{1}{4}\omega^2/\langle\omega^2\rangle$, and the normalized second invariant of the traceless strain-rate tensor (bottom row), $Q_D = \frac{1}{2}D_{ij}D_{ij}/\langle 2D_{ij}D_{ij}\rangle$. Left panels: electrons (reproduced from Paper I for completeness); and right panels: ions.

A. Energy conversion related to coherent structures

Various studies based on numerical simulations [24, 25, 27, 47–50] and solar wind data [23, 51–54] support the idea that enhanced kinetic activity, such as temperature anisotropy, heating, particle acceleration, and departures from Maxwellian velocity distributions in general, all of which commonly observed in astrophysical and laboratory plasmas, are strongly inhomogeneous. These effects are associated typically with coherent structures such as magnetic structures. Indeed, intense kinetic activity is often found in the general proximity to strong gradients, including not only magnetic, but also strong density and velocity gradients [16, 55–60]. In particular, Refs. [58, 60, 61] find that heating is correlated with both vorticity and current density, but more strongly with vorticity.

Here we are interested in looking at velocity gradients and their interaction with the pressure tensor, in view of the important role of these quantities in energy conversion in kinetic plasma, as seen in Eq. 5. We base our diagnostics on the geometric invariants of the relevant second-order tensorial quantities, an approach extensively employed in hydrodynamics to describe flow patterns [62–65]. Based on the decomposition in Eq. 11, the normalized second invariants of the traceless strain-rate matrix (D_{ij}) and the rotation-rate matrix (Ω_{ij}) are $Q_D = \frac{1}{2}D_{ij}D_{ij}/\langle 2D_{ij}D_{ij} \rangle$ and $Q_\omega = \frac{1}{4}\omega^2/\langle \omega^2 \rangle$, respectively. We can also define a similar quantity for the electric current density, say, $Q_j = \frac{1}{4}\mathbf{j}^2/\langle \mathbf{j}^2 \rangle$.

Figs. 4 and 2(b) show contours of Q_ω , Q_D and Q_j , which are found to be non-uniformly distributed in space. Moreover, comparison of Figs. 4, 2(b) with Fig. 3(a) reveals greatly similar patterns of $Pi-D$, Q_ω , Q_D and Q_j , as also shown in [60]. This indicates, as also described in Paper I, that these intermittent structures might be sites of enhanced energy conversion, which is consistent with various recent results [21–26, 57, 61].

We highlight the possible correlations of $Pi-D$, Q_ω , Q_D and Q_j by plotting them on cuts along the X direction. A sample of the absolute values of “ $Pi-D$ ” terms along the X direction with $Y \simeq 35d_i$ is shown in Fig. 5. One sees the spatial distributions of “ $Pi-D$ ” terms are evidently bursty, suggesting a connection to the spatial intermittency of the turbulence. A useful intermittency measure is given by the partial variance of increments (PVI) [48], $PVI(\mathbf{f}) = \frac{|\Delta \mathbf{f}|}{\sqrt{\langle |\Delta \mathbf{f}|^2 \rangle}}$, where $\Delta \mathbf{f} = \mathbf{f}(s + \Delta s) - \mathbf{f}(s)$. Here we choose a small scale lag, $\Delta s \simeq 0.2d_i = d_e$. The PVI series of bulk velocities for electrons (\mathbf{u}_e) and ions (\mathbf{u}_i) and magnetic field (\mathbf{b}) in Fig. 5 behave quite similar to “ $Pi-D$ ”, with peak values in

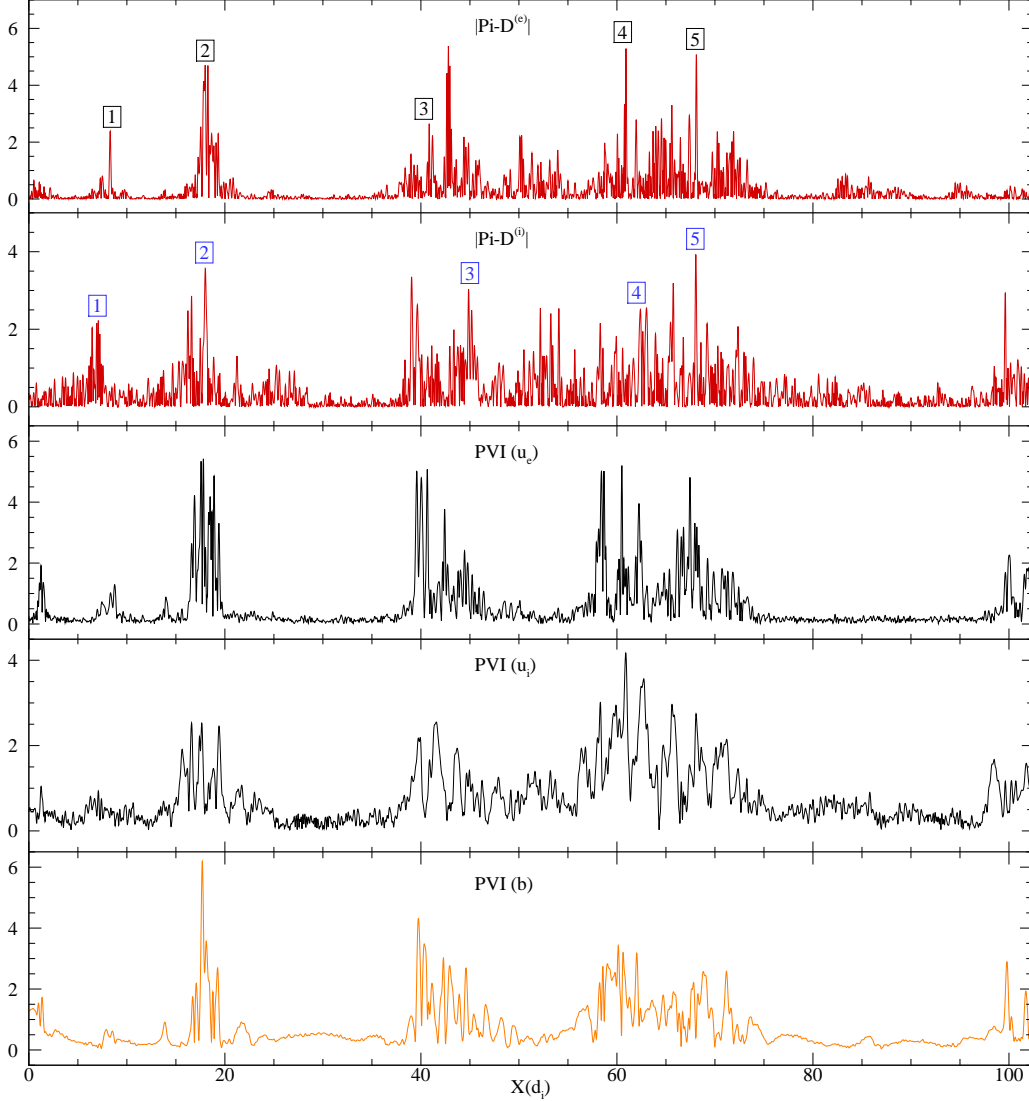


FIG. 5: Series of values on a cut ($Y \simeq 35d_i$) in X direction. (Top to bottom) absolute values of normalized “ $Pi-D$ ” for electrons; absolute values of normalized “ $Pi-D$ ” for ions; PVI values for electron bulk velocity (\mathbf{u}_e); PVI values for ion bulk velocity (\mathbf{u}_i); PVI values for magnetic field (\mathbf{b}). Events labeled by sequential numbers indicate highly intermittent regions that are enlarged below.

the vicinity of high “ $Pi-D$ ”. Events with high “ $Pi-D$ ” on the series are selected by labeling with sequential numbers in the figure, and also displayed along with Q_ω , Q_D and Q_j in Fig. 6. We might expect that intense kinetic activities are associated with current sheets, in particular, with high values of current density. In Fig. 6, however, the energy conversion through “ $Pi-D$ ” is more correlated with Q_ω and Q_D in comparison with Q_j . This can be seen

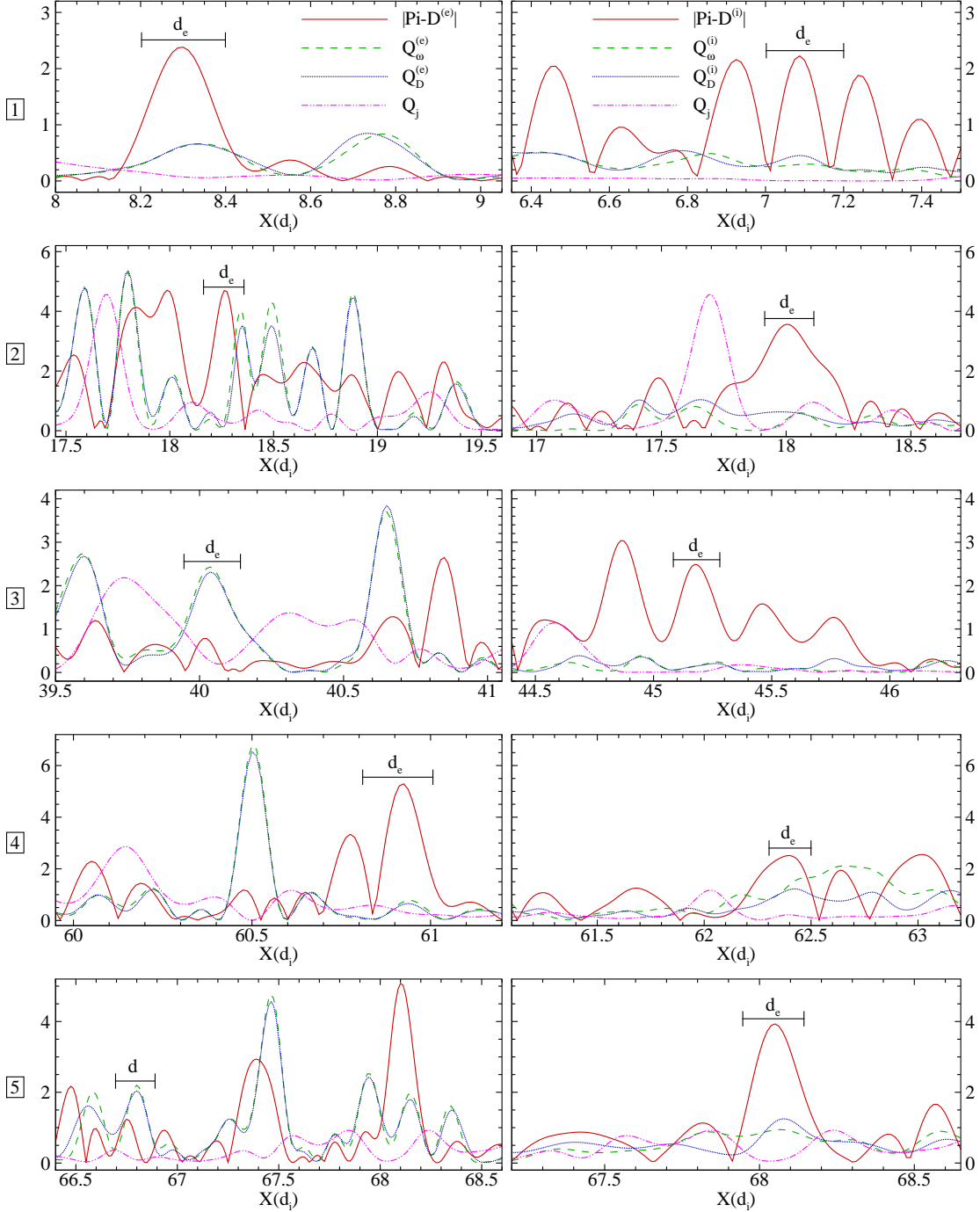


FIG. 6: Quantities, $|\Pi_{ij} D_{ij} / (-\Pi_{ij} D_{ij})_{rms}|$, Q_ω and Q_D for both (left) electrons and (right) ions, and Q_j from total current density. Top to bottom: regions labeled with 1 to 5 in Fig. 5. The black horizontal line shows the electron inertial scale d_e .

from the fluctuations for electrons in the left panels of Fig. 6, where local maxima of the absolute “ Pi - D ” terms and Q_D (or Q_ω) are close to each other, indicating a well-established

association between the symmetric and antisymmetric parts of velocity gradients and the energy conversion through the deviatoric pressure work. This result further strengthens the idea of [57–60] that energization occurs near to, but not centered on, current sheets, and that regions with large velocity gradients are prime locations for energy exchange between fields and particles.

The possible correlation between $Pi-D$ and Q_D implies more. As is well known, the viscous dissipation in HD and MHD turbulence is proportional to the mean square gradient of velocity, thus Q_D is a surrogate of the viscous dissipation in collisional fluid. This result suggests a possible resemblance between collisionless and collisional (viscous) dissipation functions. Note that the deviatoric pressure work, i.e., “ $Pi-D$ ”, differs from an irreversible dissipation mechanism, since the pointwise $Pi-D$, as shown in Fig. 3, is not positive-definite. A pointwise negative value of $Pi-D$ means that thermal (random) energy is converted into flow kinetic energy; conversely positive values of the pointwise $Pi-D$ imply a positive time rate of change of thermal (random) energy. In spite of this fundamental difference, the global energy conversion in this case is of approximately fluid-like form, which lends credence again to the idea suggested by Vasquez et al. [56], the kinetic heating of protons might be a “viscous like” process instead of a magnetic process. A possible clue comes from recent work [59] that describes in detail how the eigenvalues of the velocity gradient tensor contribute to the time derivative of the pressure tensor (see, e.g., Eq.(15) of Ref. [59]). In the light of this, one can expect “ $Pi-D$ ” to be correlated with Q_D more strongly in comparison with Q_ω , as is the case for ions in the right panels of Fig. 6.

The net effect of the deviatoric pressure work in our case is found to increase internal energy as was done by dissipation in collisional fluids. This provides a possible pathway when collisional relaxation is either absent or weak in kinetic plasma to understand how part of the fluid flow energy is converted into thermal (random) energy. To arrive at this perspective, there is no need to specify a particular mechanism, such as reconnection heating, Landau damping, cyclotron damping, or stochastic heating. Since the above commentary is based on the Vlasov equation alone, any process that contributes to the net “ $Pi-D$ ” interaction is contributing to thermal energy increase. We have also not attempted to address the question of what physical processes make such energy exchanges irreversible. Hence we cannot comment on how much of the energy converted into random motions can settle down to heat permanently. With these caveats in mind, we defer these questions to future study.

B. Joint PDFs of coherent structures

Several types of coherent structures emerge in turbulent flow, such as Q_D reflecting straining motions, Q_ω corresponding to rotation and Q_j related to magnetic discontinuities. All of them can interact with one another. Fig. 7 shows the joint PDFs $P(x, y)$.

Generally, in many hydrodynamic turbulent flows, the dominant structures are found to be tube-like structures, like vortex tubes with concentrated enstrophy (mean square vorticity), whereas sheet-like structures between these tubes are regions of dissipation. It is therefore expected that strain rate is not correlated with rotation rate. In hydrodynamic turbulence away from walls [67, 68], the joint PDF of Q_D versus Q_ω is spread very broadly. However, here the joint PDFs $P(Q_\omega, Q_D)$ in Fig. 7 are dominated by a population near the $Q_D = Q_\omega$ line, which demonstrate the strong correlation between these two quantities. It also indicates a frequently occurring class of sheet-like rather than tube-like structures, a feature consistent with many visualizations of MHD turbulence [69]. We also find that the correlation between Q_D and Q_ω for electrons (see Fig. 7(a.1)) is stronger than that for ions (see Fig. 7(a.2)). Meanwhile, Fig. 6 confirms that the curves of Q_D and Q_ω for electrons almost overlap, while those for ions are more dispersed.

The joint PDFs of Q_j versus Q_D and Q_ω , shown in Fig. 7, are spread rather broadly, indicating weak pointwise correlation between these quantities. By examining the curl of the Lorentz force, one may deduce [60, 70] that the vorticity structures tend to form on the flanks of strong current structures. Therefore, the vorticity distribution does not correlate exactly with the current, but are somewhat offset in space, but nevertheless located in the vicinity of the current. This can be also observed in Fig. 6.

V. ENERGY TRANSFER ACROSS SCALES

Now that the role of pressure tensor in global energy conversion is established, we turn to the hierarchy of scales and seek to find clues to how energy cascade proceeds from MHD scales down to the kinetic scales. A low-pass spatial filter approach [71] eliminates information at small scales without affecting remaining information at large scales, thus providing a powerful technique to study cross-scale energy transfer.

Extension of the filtering approach to kinetic plasma is technically easy. More derivation

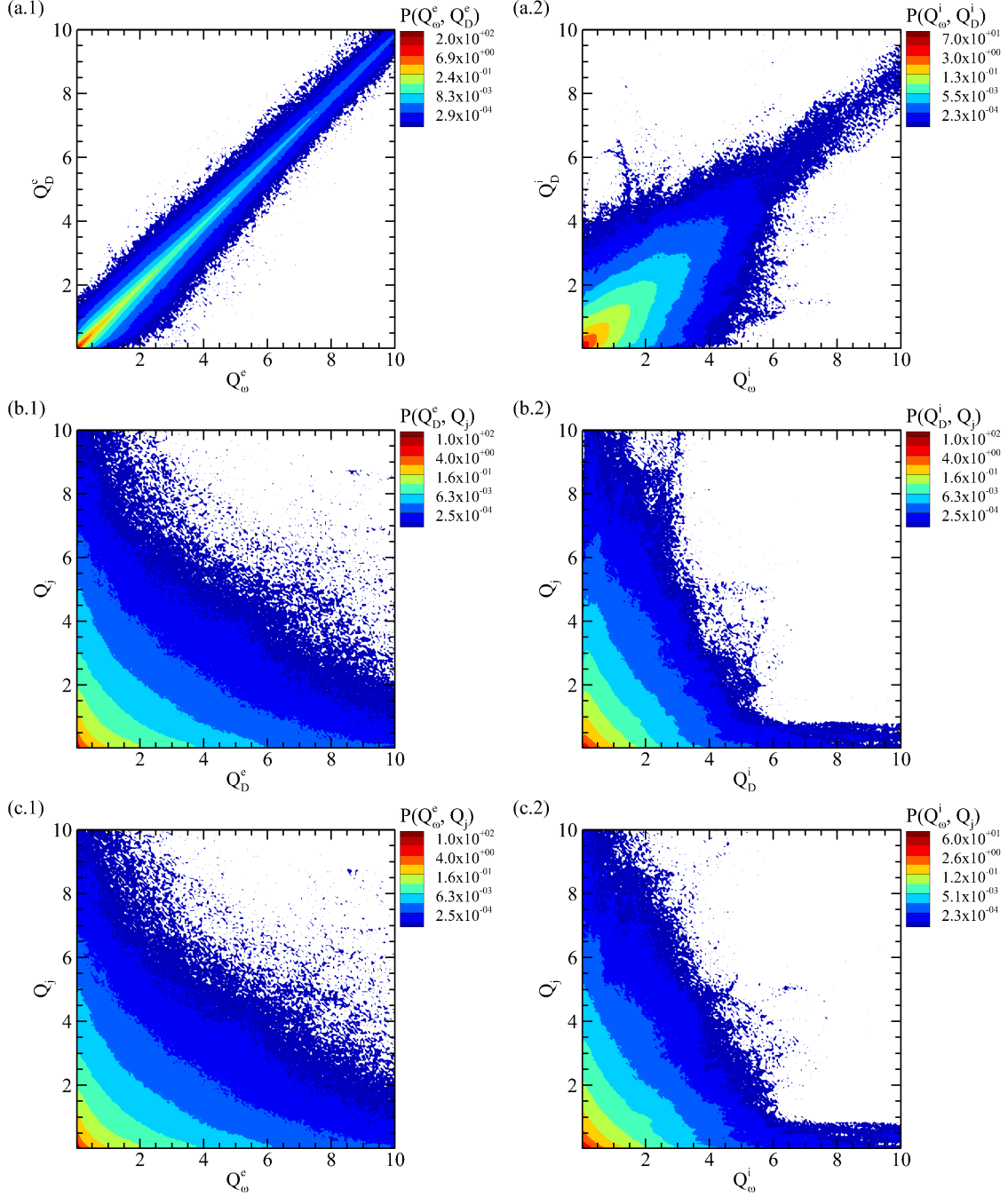


FIG. 7: Joint PDFs $P(x, y)$ of the normalized second invariants of rotation-rate, traceless strain-rate tensors, and current density, i.e., $Q_\omega = \frac{1}{4}\omega^2/\langle\omega^2\rangle$, $Q_D = \frac{1}{2}D_{ij}D_{ij}/\langle 2D_{ij}D_{ij}\rangle$, and $Q_j = \frac{1}{4}\mathbf{j}^2/\langle\mathbf{j}^2\rangle$, for both electrons (left panel) and ions (right panel). The correlation between Q_ω and Q_D is strong, for both electrons and ions, indicating sheet-like vortex structures. Meanwhile, this correlation for electrons is stronger than that for ions. The correlation between Q_ω (or Q_D) and Q_j is weak.

details can be found in App. A. Note that for conciseness of notation, the filtering scale ℓ is not written explicitly unless necessary for clarity. The equation of filtered fluid flow energy, $\tilde{E}_\alpha^f = \bar{\rho}_\alpha \tilde{\mathbf{u}}_\alpha^2/2$, can be written as

$$\partial_t \tilde{E}_\alpha^f + \nabla \cdot \mathbf{J}_\alpha^u = -\Pi_\alpha^{uu} - \Phi_\alpha^{uT} - \Lambda_\alpha^{ub}. \quad (13)$$

The meaning of each term can be understood referring to Eqs. 7-9 as:

$\mathbf{J}_\alpha^u = \tilde{E}_\alpha^f \tilde{\mathbf{u}}_\alpha + \bar{\rho}_\alpha \tilde{\boldsymbol{\tau}}_\alpha^u \cdot \tilde{\mathbf{u}}_\alpha + \bar{\mathbf{P}}_\alpha \cdot \tilde{\mathbf{u}}_\alpha$ is the spatial transport;

$\Pi_\alpha^{uu} = -(\bar{\rho}_\alpha \tilde{\boldsymbol{\tau}}_\alpha^u \cdot \nabla) \cdot \tilde{\mathbf{u}}_\alpha - q_\alpha \bar{n}_\alpha \tilde{\boldsymbol{\tau}}_\alpha^b \cdot \tilde{\mathbf{u}}_\alpha$, where $\tilde{\boldsymbol{\tau}}_\alpha^u = (\widetilde{\mathbf{u}_\alpha \mathbf{u}_\alpha} - \tilde{\mathbf{u}}_\alpha \tilde{\mathbf{u}}_\alpha)$ and $\tilde{\boldsymbol{\tau}}_\alpha^b = (\widetilde{\mathbf{u}_\alpha \times \mathbf{B}} - \tilde{\mathbf{u}}_\alpha \times \tilde{\mathbf{B}})$, is the flux of the fluid flow energy transfer across scales (if the filter scale is set to zero, these terms vanish);

$\Phi_\alpha^{uT} = -(\bar{\mathbf{P}}_\alpha \cdot \nabla) \cdot \tilde{\mathbf{u}}_\alpha$ is the fluid flow energy converted into thermal (random) energy due to pressure work;

$\Lambda_\alpha^{ub} = -q_\alpha \bar{n}_\alpha \tilde{\mathbf{E}} \cdot \tilde{\mathbf{u}}_\alpha$ is the rate of fluid flow energy conversion into electromagnetic energy, i.e., electromagnetic work done on the fluid (seen more clearly in the filtered equation for electromagnetic energy in App. B).

A. Energy fluxes

We show energy fluxes, $\langle \Pi_\alpha^{uu} \rangle$, $\langle \Phi_\alpha^{uT} \rangle$ and $\langle \Lambda_\alpha^{ub} \rangle$ varying with filtering scales in Fig. 8. The positive $\langle \Pi_\alpha^{uu} \rangle$ transfers fluid flow energy from large to small scales (i.e., a forward cascade) due to the interaction of sub-grid scales with large scales, such as the sub-scale stresses (SGS) $\tilde{\boldsymbol{\tau}}_\alpha^u = (\widetilde{\mathbf{u}_\alpha \mathbf{u}_\alpha} - \tilde{\mathbf{u}}_\alpha \tilde{\mathbf{u}}_\alpha)$ and $\tilde{\boldsymbol{\tau}}_\alpha^b = (\widetilde{\mathbf{u}_\alpha \times \mathbf{B}} - \tilde{\mathbf{u}}_\alpha \times \tilde{\mathbf{B}})$. The flow energy cascade proceeds from the largest scales (here we calculate up to the correlation scale) and transfer is sustained down to electron inertial scale d_e . The classical theory [72] in incompressible hydrodynamics suggests an energy cascade where energy is transferred from large to small scales at a constant rate. This issue has been studied in compressible HD and MHD, and the SGS energy flux is found to be approximately constant; see [6, 10, 73, 74]. The idealized notion of a constant cascade rate is not applicable here, likely due to the limited scale separation, equivalent to a relatively low Reynolds number.

Unlike the term $\langle \Pi_\alpha^{uu} \rangle$ associated with interactions between scales $> \ell$ and $< \ell$, the terms $\langle \Phi_\alpha^{uT} \rangle = \langle -(\bar{\mathbf{P}}_\alpha \cdot \nabla) \cdot \tilde{\mathbf{u}}_\alpha \rangle$ and $\langle \Lambda_\alpha^{ub} \rangle = \langle -q_\alpha \bar{n}_\alpha \tilde{\mathbf{E}} \cdot \tilde{\mathbf{u}}_\alpha \rangle$ incorporate information only from scales $> \ell$. Therefore, they are cumulative quantities. Note that $\langle \Phi_\alpha^{uT} \rangle$ is vanishingly small

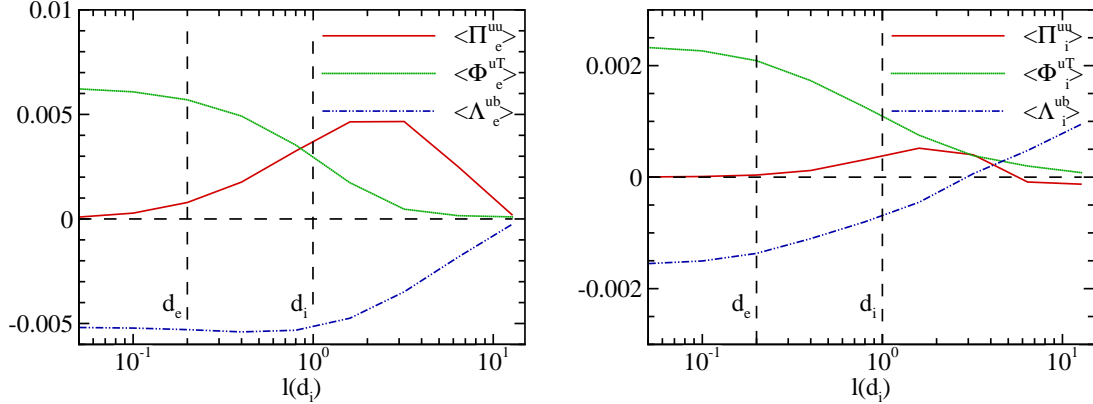


FIG. 8: Electron (left panel) and ion (right panel) energy transfer fluxes, $\langle \Pi_\alpha^{uu} \rangle$ (red solid line) between small-scale and large-scale fluid flows, $\langle \Phi_\alpha^{uT} \rangle$ (green dashed line) between fluid flow and random component, and $\langle \Lambda_\alpha^{ub} \rangle$ (blue dash-dotted line) between fluid flow and magnetic field, as a function of filtering length ℓ .

at large scales, and increases as the filter scale approaching the small scales. This indicates that the energy conversion between fluid flow and random motion by $\langle \Phi_\alpha^{uT} \rangle$ is dominated by the contribution from kinetic scales. Note that this term is the filtered version of the pressure dilatation and Pi - D terms discussed in Secs. II and IV.

In contrast, $\langle \Lambda_\alpha^{ub} \rangle$, the filtered contribution to $\langle -\mathbf{j}_\alpha \cdot \mathbf{E} \rangle$, is fairly constant over kinetic scales, and the observed increases are concentrated at a few times ion inertial scale d_i . Therefore contributions to the energy conversion between fluid flow and electromagnetic fields mainly result from the large scales in this simulation. Simulation with larger size is required to conclude if this transfer is macroscopic. We schematically represent this qualitative analysis in Fig. 9.

B. Location of energy transfer enhancement

In analogy with the pressure work Pi - D in Fig. 3(a) and coherent structures in Figs. 4, we portray spatial contours of energy flux Π_α^{uu} in Fig. 10. It is apparent that the energy flux is highly inhomogeneous. Comparing these figures, it is apparent that there is quite a significant coincidence between the coherent structures and the sites of enhanced energy transfer. Arguments have been made in favor of the hierarchy of coherent structures (see [50]). It also appears clearly in Fig. 10. In comparing the top row with $\ell \sim 2d_e$ and the

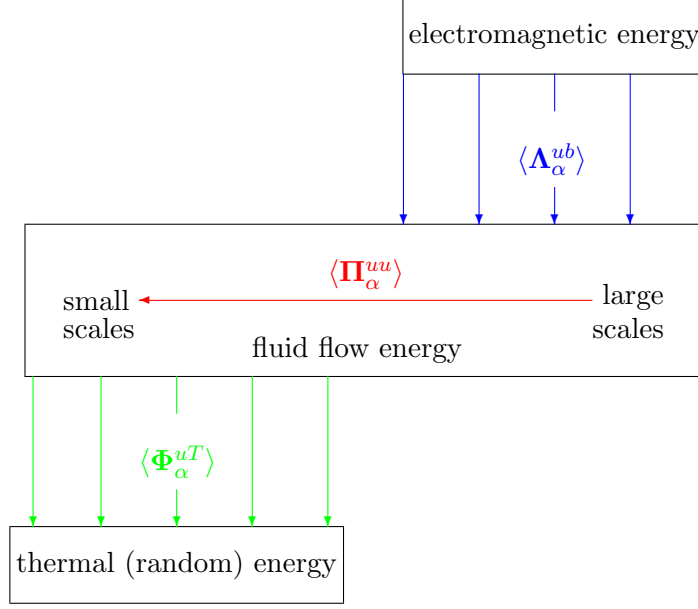


FIG. 9: Schematic diagram of energy transfer across spatial scales. Electromagnetic energy is converted into both electron and ion fluid flows at large scales due to electromagnetic work. Pressure work converts these flows into random kinetic energies at small scales. They are bridged by fluid flow energy transfer (turbulent spectral transfer) across all spatial scales.

bottom row with $\ell \sim 2d_i$, the enhanced energy transfer spots with $\ell \sim 2d_i$ are relatively broader.

VI. CONCLUSION

Global energy equations derived from the Vlasov-Maxwell system indicate the crucial role of the pressure tensor in transforming fluid flow energy into thermal (random) energy. Accordingly for each species the electromagnetic work $\mathbf{J} \cdot \mathbf{E}$, converts energy between electromagnetic fields and fluid flow energy, with a net transfer into particle flows. Finally the nonlinear transfer of energy across scales, or the standard turbulence spectral transfer, provides a more familiar coupling from large to small scales. Taken together these quantities provide a useful and essential vocabulary for describing kinetic turbulence and dissipation, and here we have provided some basic information about these processes based on global, correlation and scale filtered analysis of simulations.

The remarkable connection between the pressure work $-\Pi_{ij}D_{ij}$ (Pi - D) and the normalized

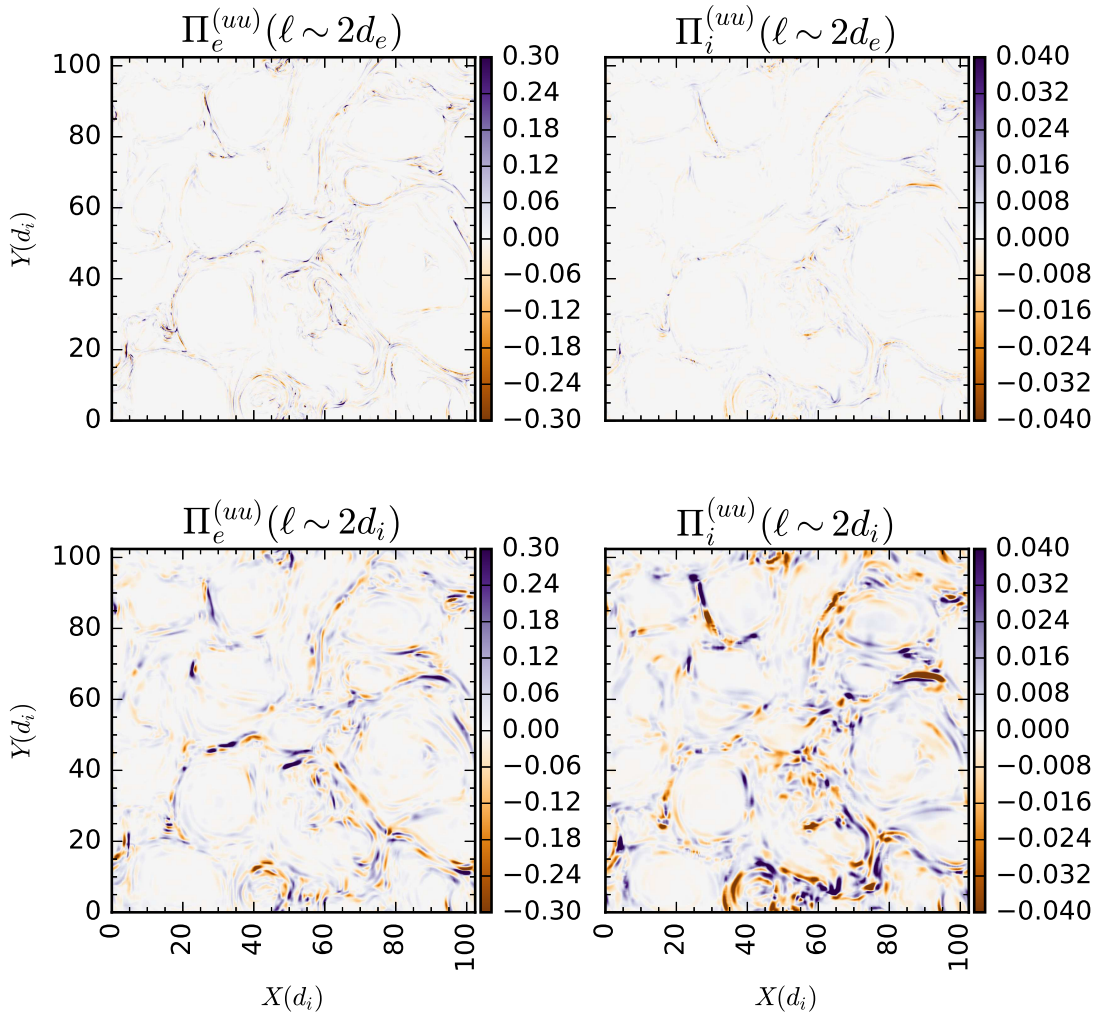


FIG. 10: Contours of species fluid flow energy transfer, Π_α^{uu} , across scales $\ell \sim 2d_e$ (top row) and $\ell \sim 2d_i$ (bottom row) for both electrons (left panel) and ions (right panel).

second invariant of the traceless strain-rate tensor $Q_D = \frac{1}{2}D_{ij}D_{ij}/\langle 2D_{ij}D_{ij} \rangle$ is supported by the substantially similar patterns of contour maps and cuts along the X direction, which corroborates again the idea suggested in Paper I. In collisional fluid, Q_D characterizes the viscous dissipation. The energy transformation by $\langle -\Pi_{ij}D_{ij} \rangle$ in our case behaves like viscous dissipation. We note that there is not any known quantitative theory to explain this strong dependence rigorously as far as we are aware. As described, for example, by Del Sarto et al. [59] and Cerri et al. [75], velocity shear provides an effective mechanism that can cause an initially isotropic pressure to become nongyrotropic, which can trigger a rich variety of inhomogeneous instabilities and nonlinear effects [57]. This might be of some help to

understand the result. Further confirmation, based on different codes, initial conditions, parameters and so on, is needed to assert any degree of universality of this result. Once it is clarified, we might find a pathway (perhaps a “viscous-like collisionless dissipation”) by which various processes act in concert and finally lead to intermittent heating. It is noteworthy that this result is in some ways complementary to the recent finding [27, 38] that in several types of kinetic simulations of plasma turbulence, conditional averages of $\mathbf{j} \cdot \mathbf{E}$ based on local values of \mathbf{j} behave very similarly to what would be expected if $\mathbf{j} \propto \mathbf{E}$, which is exact for MHD, but does not emerge in any obvious way for a kinetic plasma. These results represent a significant challenge to understand based on theory, and also provide guidance for developing phenomenological theories of plasma turbulence and dissipation.

Here we also introduced several energy transfer functions using filtering approaches to analyze their statistical properties. This approach affords a path to understand how classical cascade theory is extended from MHD scales down to kinetic scales. One can envision that energy exchange between fluid flow and magnetic and electric fields through $\langle \mathbf{E} \cdot \mathbf{j}_\alpha \rangle$ occurs at large scales, and a part of fluid flow energy is converted into internal energy through $\langle -(\mathbf{P}_\alpha \cdot \nabla) \cdot \mathbf{u}_\alpha \rangle$ at small scales. These two conversions are bridged by the fluid flow energy cascade at moderate scales.

Another important aspect of plasma turbulence and energy conversion that we have described here is the association between energy cascade, conversion processes and coherent structures. It transpires that energy transfer and conversion are in general inhomogeneous localized processes, correlated with several types of structures, such as velocity gradients (i.e., symmetric straining and vortex) and current sheets. Conversion into random energy, in effect, dissipation, is more strongly correlated with velocity gradients. This situation is actually very complex, involving a high correlation between symmetric straining and vorticity, which requires special conditions such as sheet-like structures. Conversely a weak correlation is found between current sheets and vorticity (or symmetric straining), even though these quantities are concentrated in juxtaposed regions of space. Clearly, more work is required to reveal the dynamical interactions among these coherent structures. For this, we might gain some inspiration from Refs. [60, 70] or the evolution equation of enstrophy for incompressible MHD,

$$d_t \left(\frac{1}{2} \omega^2 \right) = \omega \cdot \mathbf{D} \cdot \omega + \nu \omega \cdot \Delta \omega + \omega \cdot \nabla \times (\mathbf{j} \times \mathbf{B}) \quad (14)$$

The 2.5D simulation used in this paper presents some limitations with regard to potential generality of the conclusions. In fact the present analysis might miss some important effects present in 3D geometry (in spite of recently reported qualitatively similarities [38, 76, 77]). The intent here is not to accommodate all the dynamical complexity of the astrophysical plasma, but to propose an alternative pathway to study turbulence and heating in a kinetic plasma. Further development of these ideas may be useful, e.g., in theoretical study of coronal heating and acceleration of solar wind. Finally, neither the detailed differences between electron and ion dynamics, nor its implications for heating in space plasmas, are discussed here, but rather deferred for later study.

ACKNOWLEDGMENTS

This research was partially supported by AGS-1460130 (SHINE), NASA grants NNX14AI63G (Heliophysics Grand Challenge Theory), the Solar Probe Plus science team (ISOIS/SWRI subcontract No. D99031L), and by the MMS Theory and Modeling team, NNX14AC39G. We acknowledge support provided by the China Scholarship Council during a visit of Yan Yang to the University of Delaware.

Appendix A: Filtered fluid flow energy equation

Consider the Vlasov equation,

$$\partial_t f_\alpha + \mathbf{v} \cdot \nabla f_\alpha + \frac{q_\alpha}{m_\alpha} (\mathbf{E} + \mathbf{v} \times \mathbf{B}) \cdot \nabla_{\mathbf{v}} f_\alpha = 0. \quad (\text{A1})$$

The spatially filtered f_α is given by

$$\bar{f}_\alpha(\mathbf{x}, \mathbf{v}, t) = \int f_\alpha(\mathbf{x}', \mathbf{v}, t) G_\ell(\mathbf{x} - \mathbf{x}') d\mathbf{x}', \quad (\text{A2})$$

where $G_\ell(\mathbf{r}) = \ell^{-3} G(\mathbf{r}/\ell)$ is a filtering kernel and $G(\mathbf{r})$ is a normalized boxcar window function. The low-pass filtered \bar{f}_α only contains information at length scales $> \ell$. The filtering operation can commute with derivative operations, i.e.,

$$\overline{\partial_t f_\alpha} = \partial_t \bar{f}_\alpha, \quad \overline{\nabla f_\alpha} = \nabla \bar{f}_\alpha, \quad \overline{\nabla_{\mathbf{v}} f_\alpha} = \nabla_{\mathbf{v}} \bar{f}_\alpha. \quad (\text{A3})$$

Then the spatially filtered Vlasov equation is written as:

$$\partial_t \bar{f}_\alpha + \mathbf{v} \cdot \nabla \bar{f}_\alpha + \frac{q_\alpha}{m_\alpha} \nabla_{\mathbf{v}} \cdot (\overline{\mathbf{E} f_\alpha} + \mathbf{v} \times \overline{\mathbf{B} f_\alpha}) = 0. \quad (\text{A4})$$

From Eq. A4, moment equations for each species yields

$$\partial_t \bar{\rho}_\alpha + \nabla \cdot (\bar{\rho}_\alpha \mathbf{u}_\alpha) = 0, \quad (\text{A5})$$

$$\partial_t (\bar{\rho}_\alpha \mathbf{u}_\alpha) + \nabla \cdot (\bar{\rho}_\alpha \mathbf{u}_\alpha \mathbf{u}_\alpha) = -\nabla \cdot \bar{\mathbf{P}}_\alpha + q_\alpha (\bar{n}_\alpha \bar{\mathbf{E}} + \overline{n_\alpha \mathbf{u}_\alpha \times \mathbf{B}}). \quad (\text{A6})$$

One can see that these equations can also be derived immediately from the macroscopic Eqs. 1 and 2. A Favre-filtered (density-weighted-filtered) field [78] is defined as

$$\tilde{\mathbf{a}} = \overline{n\mathbf{a}}/\bar{n}. \quad (\text{A7})$$

Then the moment equations aforementioned can be written as

$$\partial_t \bar{\rho}_\alpha + \nabla \cdot (\bar{\rho}_\alpha \tilde{\mathbf{u}}_\alpha) = 0, \quad (\text{A8})$$

$$\partial_t (\bar{\rho}_\alpha \tilde{\mathbf{u}}_\alpha) + \nabla \cdot (\bar{\rho}_\alpha \tilde{\mathbf{u}}_\alpha \tilde{\mathbf{u}}_\alpha) = -\nabla \cdot (\bar{\rho}_\alpha \tilde{\boldsymbol{\tau}}_\alpha^u) - \nabla \cdot \bar{\mathbf{P}}_\alpha + q_\alpha \bar{n}_\alpha \left(\tilde{\mathbf{E}} + \widetilde{\mathbf{u}_\alpha \times \mathbf{B}} \right), \quad (\text{A9})$$

where $\tilde{\boldsymbol{\tau}}_\alpha^u = \left(\widetilde{\mathbf{u}_\alpha \mathbf{u}_\alpha} - \tilde{\mathbf{u}}_\alpha \tilde{\mathbf{u}}_\alpha \right)$. Eq. A9 dot product $\tilde{\mathbf{u}}_\alpha$, we can get the equation of filtered fluid flow energy $\tilde{E}_\alpha^f = \bar{\rho}_\alpha |\tilde{\mathbf{u}}_\alpha|^2/2$,

$$\begin{aligned} \partial_t \tilde{E}_\alpha^f + \nabla \cdot \left(\tilde{E}_\alpha^f \tilde{\mathbf{u}}_\alpha + \bar{\rho}_\alpha \tilde{\boldsymbol{\tau}}_\alpha^u \cdot \tilde{\mathbf{u}}_\alpha + \bar{\mathbf{P}}_\alpha \cdot \tilde{\mathbf{u}}_\alpha \right) &= (\bar{\rho}_\alpha \tilde{\boldsymbol{\tau}}_\alpha^u \cdot \nabla) \cdot \tilde{\mathbf{u}}_\alpha + q_\alpha \bar{n}_\alpha \tilde{\boldsymbol{\tau}}_\alpha^b \cdot \tilde{\mathbf{u}}_\alpha + \\ & \left(\bar{\mathbf{P}}_\alpha \cdot \nabla \right) \cdot \tilde{\mathbf{u}}_\alpha + q_\alpha \bar{n}_\alpha \tilde{\mathbf{E}} \cdot \tilde{\mathbf{u}}_\alpha, \end{aligned} \quad (\text{A10})$$

where $\tilde{\boldsymbol{\tau}}_\alpha^b = \left(\widetilde{\mathbf{u}_\alpha \times \mathbf{B}} - \tilde{\mathbf{u}}_\alpha \times \tilde{\mathbf{B}} \right)$. We can use simple notations as defined in the text following Eq. 13:

$\mathbf{J}_\alpha^u = \tilde{E}_\alpha^f \tilde{\mathbf{u}}_\alpha + \bar{\rho}_\alpha \tilde{\boldsymbol{\tau}}_\alpha^u \cdot \tilde{\mathbf{u}}_\alpha + \bar{\mathbf{P}}_\alpha \cdot \tilde{\mathbf{u}}_\alpha$ is the spatial transport;

$\mathbf{\Pi}_\alpha^{uu} = -(\bar{\rho}_\alpha \tilde{\boldsymbol{\tau}}_\alpha^u \cdot \nabla) \cdot \tilde{\mathbf{u}}_\alpha - q_\alpha \bar{n}_\alpha \tilde{\boldsymbol{\tau}}_\alpha^b \cdot \tilde{\mathbf{u}}_\alpha$ is the flux of large-scale fluid flow energy transferred to sub-scale fluid flow energy;

$\mathbf{\Phi}_\alpha^{uT} = -(\bar{\mathbf{P}}_\alpha \cdot \nabla) \cdot \tilde{\mathbf{u}}_\alpha$ is the rate of fluid flow energy converted into thermal (random) energy;

$\mathbf{\Lambda}_\alpha^{ub} = -q_\alpha \bar{n}_\alpha \tilde{\mathbf{E}} \cdot \tilde{\mathbf{u}}_\alpha$ is the rate of fluid flow energy converted into electromagnetic energy.

Appendix B: Filtered electromagnetic energy equation

From Maxwell's equations, we can obtain the equation for filtered electromagnetic energy

$$\bar{E}^m = \frac{1}{8\pi} (|\bar{\mathbf{B}}|^2 + |\bar{\mathbf{E}}|^2),$$

$$\partial_t \bar{E}^m + \frac{c}{4\pi} \nabla \cdot (\bar{\mathbf{E}} \times \bar{\mathbf{B}}) = -\bar{\mathbf{E}} \cdot \bar{\mathbf{j}}, \quad (\text{B1})$$

Taking the electromagnetic work (i.e., Λ_α^{ub} in Eqs. 13 and A10) as a source in Eq. B1 yields

$$\partial_t \bar{E}^m + \frac{c}{4\pi} \nabla \cdot (\bar{\mathbf{E}} \times \bar{\mathbf{B}}) = \sum_\alpha q_\alpha \bar{n}_\alpha (\tilde{\mathbf{E}} - \bar{\mathbf{E}}) \cdot \tilde{\mathbf{u}}_\alpha - \sum_\alpha q_\alpha \bar{n}_\alpha \tilde{\mathbf{E}} \cdot \tilde{\mathbf{u}}_\alpha, \quad (\text{B2})$$

which can be written as

$$\partial_t \bar{E}^m + \nabla \cdot \mathbf{J}^b = - \sum_\alpha \Pi_\alpha^{bb} + \sum_\alpha \Lambda_\alpha^{ub}, \quad (\text{B3})$$

where

$\mathbf{J}^b = \frac{c}{4\pi} (\bar{\mathbf{E}} \times \bar{\mathbf{B}})$ is the spatial transport;

$\Pi_\alpha^{bb} = -q_\alpha \bar{n}_\alpha \tilde{\boldsymbol{\tau}}_\alpha^e \cdot \tilde{\mathbf{u}}_\alpha$, where $\tilde{\boldsymbol{\tau}}_\alpha^e = (\tilde{\mathbf{E}} - \bar{\mathbf{E}})$, is the flux of electromagnetic energy across scales due to sub-scale work done by the electric field;

$\Lambda_\alpha^{ub} = -q_\alpha \bar{n}_\alpha \tilde{\mathbf{E}} \cdot \tilde{\mathbf{u}}_\alpha$, the rate of fluid flow energy conversion into electromagnetic energy, is the same as those in Eqs. 13 and A10, which is canceled out on combining Eqs. 13 (or A10) and B1. Therefore, the filtered equation for total fluid flow and electromagnetic energy takes the form

$$\partial_t \left(\sum_\alpha \tilde{E}_\alpha^f + \bar{E}^m \right) + \nabla \cdot \left(\sum_\alpha \mathbf{J}_\alpha^u + \mathbf{J}^b \right) = - \sum_\alpha \Pi_\alpha^{uu} - \sum_\alpha \Pi_\alpha^{bb} - \sum_\alpha \Phi_\alpha^{uT}, \quad (\text{B4})$$

where

$\mathbf{J}_\alpha^u = \tilde{E}_\alpha^f \tilde{\mathbf{u}}_\alpha + \bar{\rho}_\alpha \tilde{\boldsymbol{\tau}}_\alpha^u \cdot \tilde{\mathbf{u}}_\alpha + \bar{\mathbf{P}}_\alpha \cdot \tilde{\mathbf{u}}_\alpha$,

$\Pi_\alpha^{uu} = -(\bar{\rho}_\alpha \tilde{\boldsymbol{\tau}}_\alpha^u \cdot \nabla) \cdot \tilde{\mathbf{u}}_\alpha - q_\alpha \bar{n}_\alpha \tilde{\boldsymbol{\tau}}_\alpha^b \cdot \tilde{\mathbf{u}}_\alpha$ and

$\Phi_\alpha^{uT} = -(\bar{\mathbf{P}}_\alpha \cdot \nabla) \cdot \tilde{\mathbf{u}}_\alpha$ are defined in the text following Eqs. 13 and A10.

-
- [1] P. J. Coleman, *Astrophys. J.* **153**, 371 (1968).
 - [2] C. Tu, Z. Pu, and F. Wei, *J. Geophys. Res.* **89**, 9695 (1984).
 - [3] W. H. Matthaeus and M. Velli, *Space Sci. Rev.* **160**, 145 (2011).
 - [4] A. A. Schekochihin, S. C. Cowley, W. Dorland, G. W. Hammett, G. G. Howes, E. Quataert, and T. Tatsuno, *Astrophys. J. Suppl. S.* **182**, 310 (2009).
 - [5] G. G. Howes, *Phil. Trans. R. Soc. A* **373**, 20140145 (2015).
 - [6] Y. Yang, Y. Shi, M. Wan, W. H. Matthaeus, and S. Chen, *Phys. Rev. E* **93**, 061102 (2016).
 - [7] S. P. Gary, *Theory of Space Plasma Microinstabilities* (Cambridge University Press, New York, 1993).

- [8] A. A. Schekochihin, S. C. Cowley, W. Dorland, G. W. Hammett, G. G. Howes, G. G. Plunk, E. Quataert, and T. Tatsuno, *Plasma Phys. Controlled Fusion* **50**, 124024 (2008).
- [9] W. H. Matthaeus, S. Oughton, K. T. Osman, S. Servidio, M. Wan, S. P. Gary, M. A. Shay, F. Valentini, V. Roytershteyn, H. Karimabadi, and S. C. Chapman, *Astrophys. J.* **790**, 155 (2014), arXiv:1404.6569 [physics.space-ph].
- [10] H. Aluie, *Phys. Rev. Lett.* **106**, 174502 (2011).
- [11] A. A. Chernyshov, K. V. Karelsky, and A. S. Petrosyan, *Phys. Plasmas* **13**, 032304 (2006).
- [12] A. Petrosyan, A. Balogh, M. L. Goldstein, J. Léorat, E. Marsch, K. Petrovay, B. Roberts, R. von Steiger, and J. C. Vial, *Space Sci. Rev.* **156**, 135 (2010).
- [13] M. P. Martin, U. Piomelli, and G. Candler, *Theor. Comput. Fluid Dyn.* **13**, 361 (2000).
- [14] O. Agullo, W.-C. Müller, B. Knaepen, and D. Carati, *Phys. Plasmas* **8**, 3502 (2001).
- [15] M. Miesch, W. Matthaeus, A. Brandenburg, A. Petrosyan, A. Pouquet, C. Cambon, F. Jenko, D. Uzdensky, J. Stone, S. Tobias, J. Toomre, and M. Velli, *Space Sci. Rev.* **194**, 97 (2015).
- [16] S. A. Markovskii, B. J. Vasquez, C. W. Smith, and J. V. Hollweg, *Astrophys. J.* **639**, 1177 (2006).
- [17] J. V. Hollweg, *J. Geophys. Res.* **91**, 4111 (1986).
- [18] J. V. Hollweg and P. A. Isenberg, *J. Geophys. Res.* **107**, 1147 (2002).
- [19] S. P. Gary and S. Saito, *J. Geophys. Res.* **108**, 1194 (2003).
- [20] S. P. Gary, S. Saito, and H. Li, *Geophys. Res. Lett.* **35**, L02104 (2008).
- [21] P. Dmitruk, W. H. Matthaeus, and N. Seenu, *Astrophys. J.* **617**, 667 (2004).
- [22] A. Retinò, D. Sundkvist, A. Vaivads, F. Mozer, M. André, and C. J. Owen, *Nature Phys.* **3**, 235 (2007).
- [23] D. Sundkvist, A. Retinò, A. Vaivads, and S. D. Bale, *Phys. Rev. Lett.* **99**, 025004 (2007).
- [24] T. N. Parashar, S. Servidio, M. A. Shay, B. Breech, and W. H. Matthaeus, *Phys. Plasmas* **18**, 092302 (2011), 10.1063/1.3630926.
- [25] J. M. TenBarge and G. G. Howes, *Astrophys. J. Lett.* **771**, L27 (2013).
- [26] S. Perri, M. L. Goldstein, J. C. Dorelli, and F. Sahraoui, *Phys. Rev. Lett.* **109**, 191101 (2012).
- [27] M. Wan, W. H. Matthaeus, V. Roytershteyn, H. Karimabadi, T. Parashar, P. Wu, and M. Shay, *Physical Review Letters* **114**, 175002 (2015).
- [28] Y. Yang, W. H. Matthaeus, Y. Shi, M. Wan, and S. Chen, *Phys. Fluid* **29**, 035105 (2017).
- [29] S. B. Pope, *Turbulent flows*, first edition ed. (Cambridge University Press, 2000).

- [30] M. Crespo, S. Jamme, and P. Chassaing, in *Proceedings of 35th AIAA fluid dynamics conference and exhibit* (AIAA, Toronto, Ontario Canada, 2005).
- [31] S. Sarkar, *Phys. Fluids A* **4**, 2674 (1992).
- [32] H. Miura and S. Kida, *Phys. Fluids* **7**, 1732 (1995).
- [33] M. H. Lee, *Physica A* **365**, 150 (2006).
- [34] K. Lee, V. Venugopal, and S. S. Girimaji, *Phys. Scr.* **91**, 084006 (2016).
- [35] H. J. Cai and L. C. Lee, *Phys. Plasmas* **4**, 509 (1997).
- [36] L. Yin, D. Winske, S. P. Gary, and J. Birn, *Geophys. Res. Lett.* **28**, 2173 (2001).
- [37] Y. Yang, W. H. Matthaeus, T. N. Parashar, P. Wu, M. Wan, Y. Shi, S. Chen, V. Roytershteyn, and W. Daughton, *Phys. Rev. Lett.* **Under review** (2017).
- [38] M. Wan, W. H. Matthaeus, V. Roytershteyn, T. N. Parashar, P. Wu, and H. Karimabadi, *Physics of Plasmas* **23**, 042307 (2016).
- [39] J. Birn and M. Hesse, *J. Geophys. Res.* **106**, 3737 (2001).
- [40] J. Birn, M. Hesse, and K. Schindler, *Physics of Plasmas* **13**, 092117 (2006).
- [41] J. Birn and M. Hesse, *Physics of Plasmas* **17**, 012109 (2010).
- [42] A. Zeiler, D. Biskamp, J. F. Drake, B. N. Rogers, M. A. Shay, and M. Scholer, *J. Geophys. Res.* **107**, 1230 (2002).
- [43] P. Wu, M. Wan, W. H. Matthaeus, M. A. Shay, and M. Swisdak, *Phys. Rev. Lett.* **111**, 121105 (2013).
- [44] C. C. Haggerty, T. N. Parashar, W. H. Matthaeus, M. A. Shay, M. Wan, P. Wu, and S. Servidio, *In preparation* (2017).
- [45] W. G. Vincenti and C. H. Kruger, *Introduction to physical gas dynamics, by Vincenti, Walter Guido; Kruger, Charles H. New York, Wiley [1965]* (1965).
- [46] S. I. Braginskii, *Rev. Plasma Phys.* **1**, 205 (1965).
- [47] S. Servidio, F. Valentini, F. Califano, and P. Veltri, *Phys. Rev. Lett.* **108**, 045001 (2012).
- [48] A. Greco, F. Valentini, S. Servidio, and W. H. Matthaeus, *Phys. Rev. E* **86**, 066405 (2012).
- [49] M. Wan, W. H. Matthaeus, H. Karimabadi, V. Roytershteyn, M. Shay, P. Wu, W. Daughton, B. Loring, and S. C. Chapman, *Phys. Rev. Lett.* **109** (2012), 10.1103/PhysRevLett.109.195001.
- [50] H. Karimabadi, V. Roytershteyn, M. Wan, W. H. Matthaeus, W. Daughton, P. Wu, M. Shay, B. Loring, J. Borovsky, E. Leonardis, and S. C. Chapman, *Phys. Plasmas* **20**, 012303 (2013).

- [51] K. T. Osman, W. H. Matthaeus, A. Greco, and S. Servidio, *Astrophys. J. Lett.* **727**, L11 (2011).
- [52] K. T. Osman, W. H. Matthaeus, M. Wan, and A. F. Rappazzo, *Phys. Rev. Lett.* **108**, 261102 (2012).
- [53] K. T. Osman, W. H. Matthaeus, B. Hnat, and S. C. Chapman, *Phys. Rev. Lett.* **108**, 261103 (2012).
- [54] P. Wu, S. Perri, K. Osman, M. Wan, W. H. Matthaeus, M. A. Shay, M. L. Goldstein, H. Karimabadi, and S. Chapman, *Astrophys. J.* **763**, L30 (2013).
- [55] J. D. Huba, *Geophys. Res. Lett.* **23**, 2907 (1996).
- [56] B. J. Vasquez and S. A. Markovskii, *Astrophys. J.* **747**, 19 (2012).
- [57] S. Servidio, F. Valentini, D. Perrone, A. Greco, F. Califano, W. H. Matthaeus, and P. Veltri, *J. Plasma Phys.* **81**, 325810107 (2015).
- [58] L. Franci, P. Hellinger, L. Matteini, A. Verdini, and S. Landi, *AIP Conf. Proc.* **1720**, 040003 (2016).
- [59] D. Del Sarto, F. Pegoraro, and F. Califano, *Phys. Rev. E* **93**, 053203 (2016), arXiv:1507.04895 [physics.plasm-ph].
- [60] T. N. Parashar and W. H. Matthaeus, *Astrophys. J.* **832**, 57 (2016), arXiv:1610.02912 [physics.space-ph].
- [61] S. Servidio, K. T. Osman, F. Valentini, D. Perrone, F. Califano, S. Chapman, W. H. Matthaeus, and P. Veltri, *Astrophys. J.* **781**, L27 (2014).
- [62] M. S. Chong, A. E. Perry, and B. J. Cantwell, *Phys. Fluids A: Fluid Dyn.* **2**, 765 (1990).
- [63] J. Soria, R. Sondergaard, B. J. Cantwell, M. S. Chong, and A. E. Perry, *Phys. Fluids* **6**, 871 (1994).
- [64] M. S. Chong, J. Soria, A. E. Perry, J. Chacin, B. J. Cantwell, and Y. Na, *J. Fluid Mech.* **357**, 225 (1998).
- [65] A. Ooi, J. Martin, J. Soria, and M. S. Chong, *J. Fluid Mech.* **381**, 141 (1999).
- [66] H. Xu, N. T. Ouellette, and E. Bodenschatz, *Phys. Rev. Lett.* **98**, 050201 (2007).
- [67] J. Jiménez, A. A. Wary, P. G. Saffman, and R. S. Rogallo, *J. Fluid Mech.* **255**, 65 (1993).
- [68] H. M. Blackburn, N. N. Mansour, and B. J. Cantwell, *J. Fluid Mech.* **310**, 269 (1996).
- [69] V. Dallas and A. Alexakis, *Phys. Fluids* **25**, 105106 (2013).
- [70] W. H. Matthaeus, *Geophys. Res. Lett.* **9**, 660 (1982).

- [71] M. Germano, *J. Fluid Mech.* **238**, 325 (1992).
- [72] A. N. Kolmogorov, *Dokl. Akad. Nauk SSSR* **30**, 301 (1941).
- [73] H. Aluie, S. Li, and H. Li, *Astrophys. J. Lett.* **751**, L29 (2012).
- [74] J. Wang, Y. Yang, Y. Shi, Z. Xiao, X. T. He, and S. Chen, *Phys. Rev. Lett.* **110**, 214505 (2013).
- [75] S. S. Cerri, F. Pegoraro, F. Califano, D. D. Sarto, and F. Jenko, *Phys. Plasmas* **21**, 112109 (2014).
- [76] H. Karimabadi, V. Roytershteyn, W. Daughton, and Y.-H. Liu, *Space Sci. Rev.* **178**, 307 (2013).
- [77] T. C. Li, G. G. Howes, K. G. Klein, and J. M. TenBarge, *Astrophys. J. Lett.* **832**, L24 (2016).
- [78] A. Favre, in *Problems of Hydrodynamic and Continuum Mechanics* (SIAM, Philadelphia, PA, USA, 1969) pp. 231–266.